MICROSTRUCTURE OF AIR PLASMA-SPRAYED NiAl COATING ISOTHERMALLY EXPOSED AT 850 °C FOR 6 MINUTES

KAROL IŽDINSKÝ[1]*, JOZEF IVAN[1], MILINA ZEMÁNKOVÁ[1], ADRIÁN CSUBA[1], PAVOL MINÁR[1], ZITA IŽDINSKÁ[2]

The microstructure of NiAl coating formed by air plasma spraying of ball-milled NiAl30 powder, isothermally exposed at 850 °C for 6 minutes in air, is studied in this paper. An exothermic reaction starting at 490 °C was determined by DTA within the heating period performed with the rate of 10 $K \cdot min^{-1}$. The reaction was recognized as a reaction synthesis restricted to local areas with appropriate chemical and phase composition. Metallic phases with the exception of some retained γ-Ni reacted to form NiAl phase. Average hardness of the coating increased from 130 to 450 HV 0.01. The local temperature increase induced by the exothermic reaction is responsible for the complete transformation of all amorphous Al_2O_3 oxides into crystalline oxides with spinel type structure.

K e y w o r d s: NiAl coating, air-plasma spraying, microstructure, TEM studies, intermetallic phases, thermal analysis

MIKROŠTRUKTÚRA POVLAKU NiAl ZHOTOVENÉHO PLAZMOVÝM STRIEKANÍM NA VZDUCHU PO 6-MINÚTOVEJ IZOTERMICKEJ EXPOZÍCII PRI TEPLOTE 850 °C

V práci sú uvedené výsledky štúdia mikroštruktúry povlaku NiAl zhotoveného plazmovým striekaním prášku NiAl30 na vzduchu, ktorý bol pripravený mletím v guľovom mlyne, po 6-minútovej izotermickej expozícii pri teplote 850 °C. DTA odhalila exotermickú reakciu, ktorá začala prebiehať v povlaku ohrievanom rýchlosťou 10 $K \cdot min^{-1}$ pri teplote 490 °C. Ukázalo sa, že ide o reakčnú syntézu lokalizovanú do oblastí s vhodným chemickým a fázovým zložením. Kovové zložky povlaku, s výnimkou malého množstva zvyškového γ-Ni, vzájomne reagovali, pričom vznikal najmä NiAl. Priemerná tvrdosť povlaku sa tým zvýšila zo 130 na 450 HV 0,01. Lokálny nárast teploty spôsobený exotermickou reakciou

[1] Institute of Materials and Machine Mechanics, Slovak Academy of Sciences, Račianska 75, 831 02 Bratislava 3, Slovak Republic
[2] Department of Materials and Technologies, Slovak Technical University, Pionierska 15, 812 31 Bratislava 1, Slovak Republic
* corresponding author, e-mail: ummsizd@savba.sk

je zodpovedný za kompletnú transformáciu amorfných Al_2O_3 oxidov na kryštalické so štruktúrou spinelového typu.

1. Introduction

Air plasma-sprayed (APS) Ni-Al coatings unambiguously took their position in the design and performance of thermal barrier coatings. They reliably fulfil their role as oxidation-resistant metallic bond coating, providing a good thermal expansion match between the top coat and the substrate.

We have shown in our previous work [1] that ball-milled NiAl 30 powder can be successfully used to produce NiAl APS coating. However, numerous chemical and structural inhomogeneities were determined by microstructural studies. The coating was found to be formed by a mixture of phases including α-Al and γ-Ni based solid solutions, β-NiAl, martensitic NiAl, and γ'-Ni_3Al intermetallic compounds. Amorphous, partially crystallized and crystallized fine-grained Al_2O_3 oxides with spinel structure were also determined.

This microstructure is evidently far from equilibrium, and it is expected to transform when exposed to higher temperatures. The aim of this article is to present further results of microstructural studies performed on NiAl coating isothermally exposed at 850 ℃ for 6 minutes.

2. Experimental material and procedure

NiAl coating was prepared by APS of NiAl30 ball-milled nickel base binary powder [2] at a total power input of 32 kW. The details of APS process are given elsewhere [1]. As-sprayed coating was removed from the steel substrate and isothermally exposed in air at the temperature of 850 ℃ for 6 minutes. The heating rate was 10 $K \cdot min^{-1}$. The phase reactions induced by the applied thermal treatment were monitored by differential thermal analysis (DTA). The sample was subsequently removed from the furnace and cooled in air.

Light microscopy (LM) and Vickers microhardness measurements were used for structural studies. DTA analysis was performed using NETSCH STA 409 analyzer. Microstructural studies were launched by scanning electron microscopy (SEM) observations using JEOL 5310 electron microscope operated at the accelerating voltage of 15 kV.

The energy-dispersive X-ray spectroscopy (EDX) was applied for phase chemical analysis, using Kevex Delta class IV spectrometer with an ultra-thin window detector (Kevex Quantum detector). Transmission electron microscopy (TEM) analysis including bright field and dark field image observations with selected area electron diffraction (SAED), were carried out at a JEOL JEM 100 C analytical electron microscope operated at 100 kV. The thin foil preparation for TEM observations was accomplished by ion milling, using the BAL-TEC RES 010 rapid etching system.

3. Results

DTA curve obtained by heating of NiAl coating is shown in Fig. 1. One exothermic peak appearing in the temperature range from 490 °C to approximately 730 °C was detected. No distinct peak has been observed at 638 °C – the Ni-Al eutectic temperature.

The structure of the thermally treated coating is formed by heterogeneous mixture of bright matrix and darkly appearing inclusions and pores. Typical structure in the longitudinal section as revealed by light microscopy is shown in Fig. 2. Wide scattered hardness values ranging from 224 to 715 HV 0.01 were obtained by Vickers microhardness measurements. The average hardness determined from 30 measurements in the cross section of the coating was 450 HV 0.01 with the standard deviation of 180 HV 0.01.

SEM observations with EDX analysis confirmed that bright grains refer to primary γ-Ni. The major matrix is formed by regions with mostly similar atomic contents of Al and Ni. Typical microstructure in the cross-sectional view as revealed by SEM is shown in Fig. 3a. Corresponding typical EDX point spectra are presented in Figs. 3b and 3c. No regions indicating the presence of α-Al grains were observed. Darkly appearing elongated inclusions, known from previous work were repeatedly identified as aluminium oxides, sometimes containing little amounts of Ni.

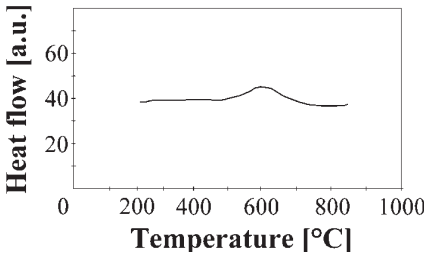

Fig. 1. DTA curve of NiAl coating heated to 850 °C in air with the heating rate of 10 $K \cdot min^{-1}$.

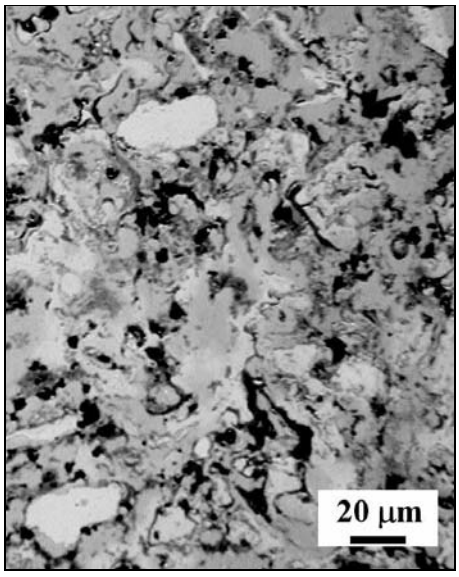

Fig. 2. Light micrograph of the longitudinal section of NiAl coating.

Fig. 3a. Microstructure in the cross-section of NiAl coating (SEM).

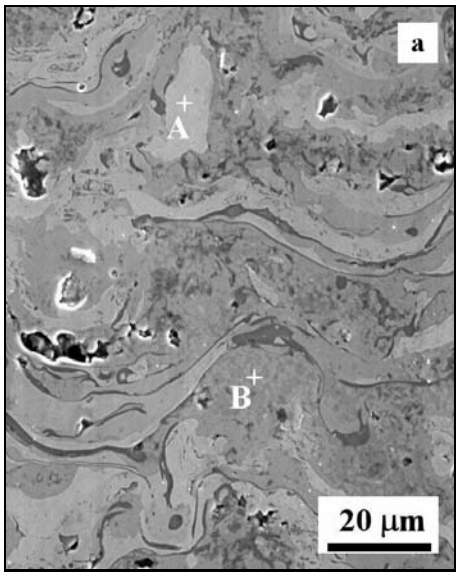

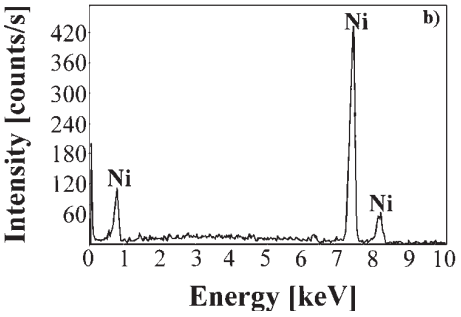

Fig. 3b. EDX spectrum acquired by point analysis at A (energy-dispersive X-ray spectroscopy).

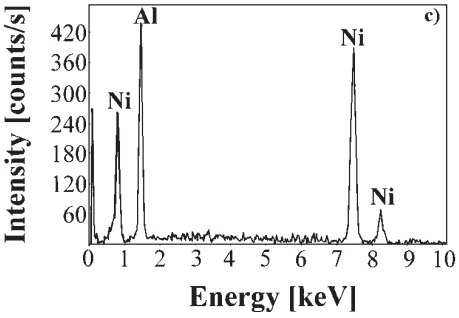

Fig. 3c. EDX spectrum acquired by point analysis at B (energy-dispersive X-ray spectroscopy).

The identification of present phases in the thermally treated coating was completed by TEM observations. Body centered cubic of the CsCl type (B2) based solid solution β-NiAl was confirmed as the predominant phase. Typical example is shown in Fig. 4. Martensitic NiAl with face-centered tetragonal Ll_0 structure displaying both acicular and plate-like twinned morphology appears quite often as shown in Figs. 5 and 6.

Grains with high Ni contents refer to face centered cubic γ-Ni based solid solu-

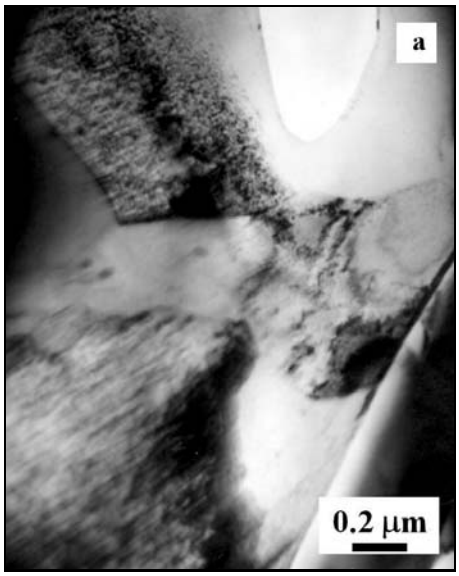

Fig. 4a. β-NiAl in the microstructure of NiAl coating (TEM, BF image).

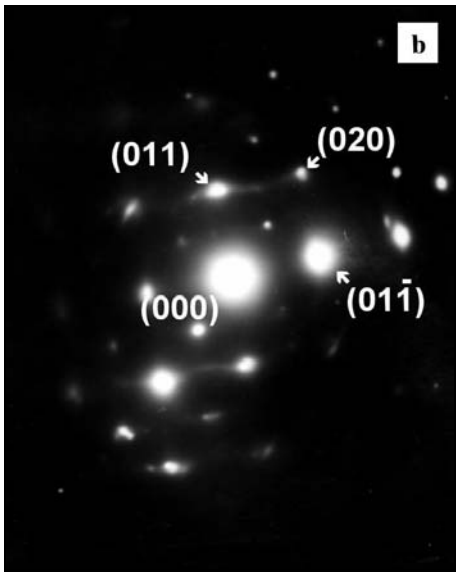

Fig. 4b. SAED pattern corresponding to [1 0 0] zone of β-NiAl.

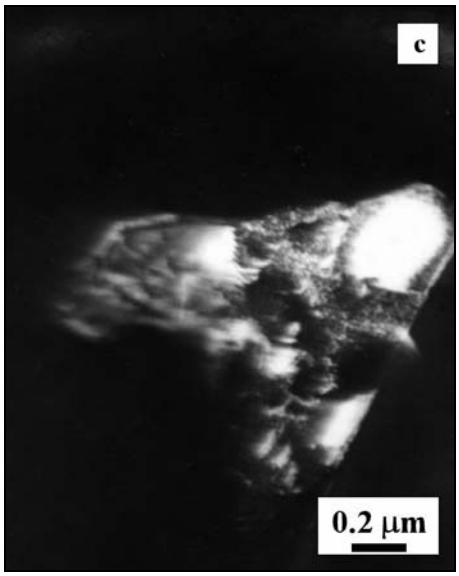

Fig. 4c. Dark field image formed using (0 1 0) reflection of β-NiAl.

tion. Twinned γ-Ni grain is shown in Fig. 7. Corresponding SAED pattern reveals (1 1 1) as the twinning plane in this particular grain. Besides β-NiAl and γ-Ni also

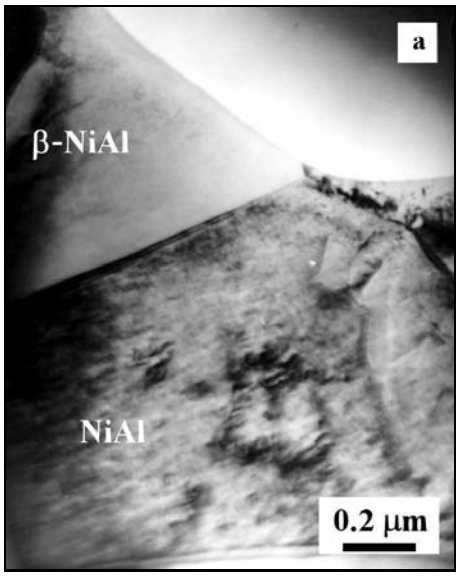

Fig. 5a. Acicular NiAl martensite in the microstructure of NiAl coating (TEM, BF image).

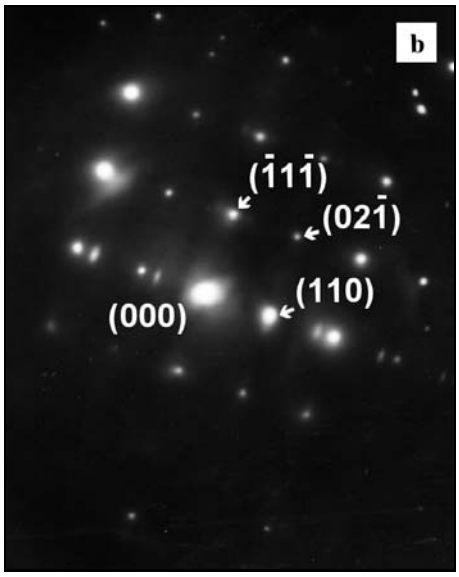

Fig. 5b. SAED pattern corresponding to $[\bar{1}\,1\,2]$ zone of martensitic NiAl.

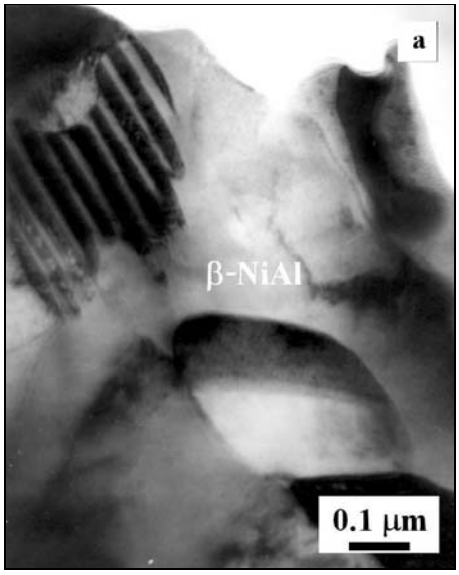

Fig. 6a. Plate-like martensitic NiAl neighbouring β-NiAl (TEM, BF image).

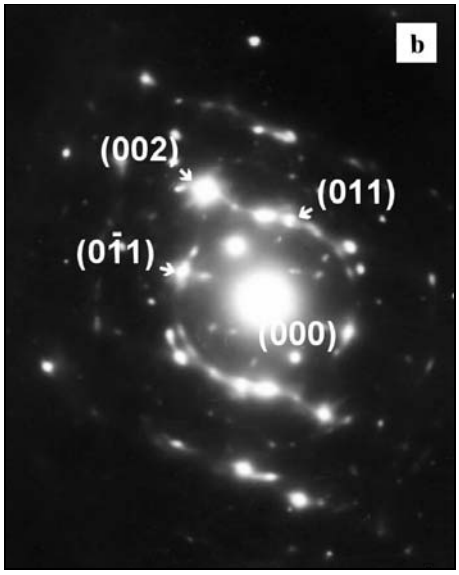

Fig. 6b. SAED pattern corresponding to $[1\,0\,0]$ zone of β-NiAl.

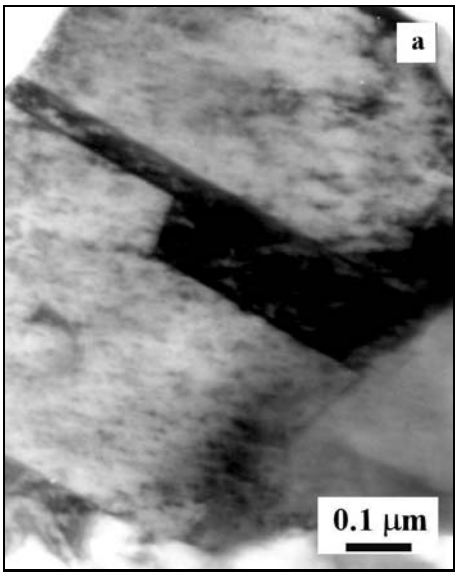

Fig. 7a. Twinned γ-Ni grain in the microstructure of NiAl coating (TEM, BF image).

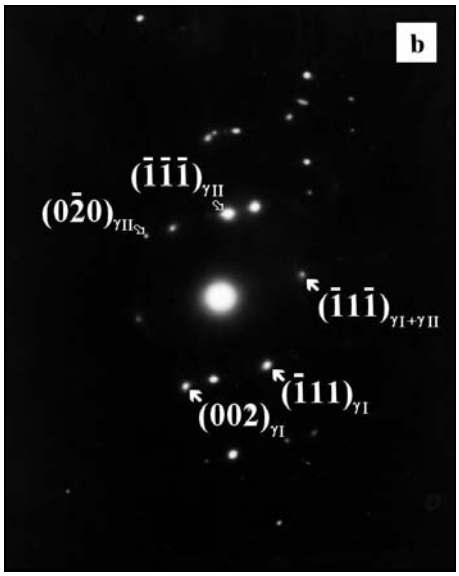

Fig. 7b. SAED patterns corresponding to $[\bar{1}\,\bar{1}\,0]$ zone of γ-Ni_I superimposed on $[\bar{1}\,0\,1]$ zone of γ-Ni_{II}.

orthorhombic of the $D0_{20}$ type Al_3Ni and Cu_3Au (Ll2) type γ'-Ni_3Al intermetallics were observed in the microstructure. However, their frequency of appearance was very low. Distinct orientation relationship between Al_3Ni and β-NiAl was observed as shown in Fig. 8. It can be expressed as follows:

$$(1\,\bar{2}\,1)_{Al_3Ni} \| (0\,1\,0)_{\beta\text{-NiAl}} \wedge [\bar{2}\,\bar{1}\,0]_{Al_3Ni} \| [1\,0\,1]_{\beta\text{-NiAl}}.$$

γ'-Ni_3Al intermetallic was observed without any distinctive morphology as presented in Fig. 9.

Strictly saying, no amorphous oxides were observed in the analysed microstructure. Just crystalline oxides with spinel type structure can be found in the thermally treated coating. Monocrystallic as well as ring SAED patterns could have been obtained. Typical example with monocrystallic SAED pattern is shown in Fig. 10.

4. Discussion of results

Light microscopy observations did not reveal any dramatic change in the appearance of thermally treated microstructure, when compared with NiAl APS coating [1]. It looks that slight increase in porosity took place within the applied thermal treatment, however no targeted quantification was performed in this work.

Fig. 8a. β-NiAl grain with small Al_3Ni particles (TEM, BF image).

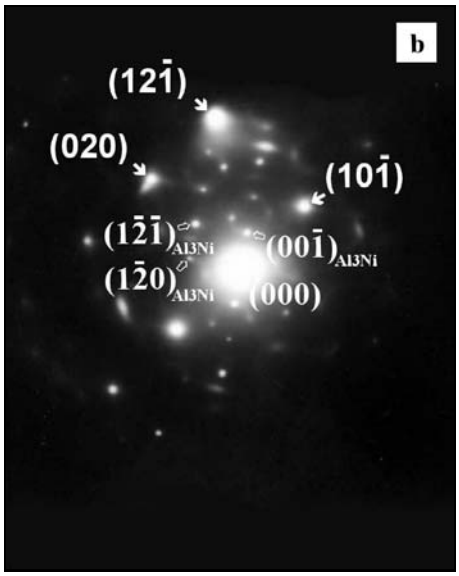

Fig. 8b. SAED patterns corresponding to [1 0 1] zone of β-NiAl superimposed on [$\bar{2}\,\bar{1}$ 0] zone of Al_3Ni.

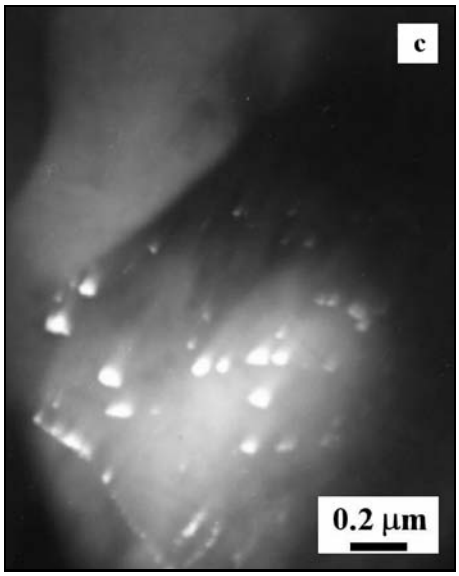

Fig. 8c. Dark field image formed using (0 0 $\bar{1}$) reflection of Al_3Ni.

DTA clearly confirmed an exothermic reaction running within the heating period. This is in agreement with our previous assumptions that phase transform-

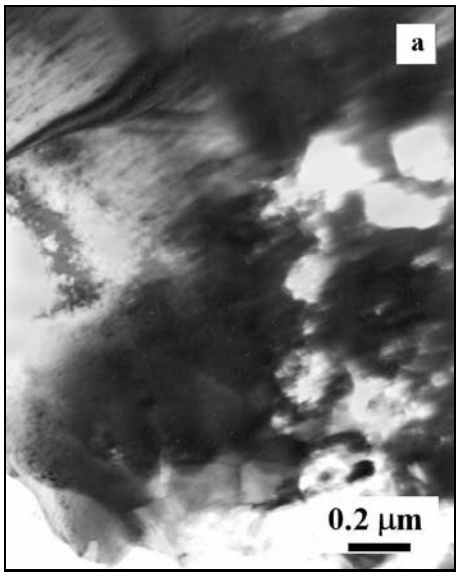

Fig. 9a. γ-Ni/γ'-Ni_3Al in the microstructure of NiAl coating (TEM, BF image).

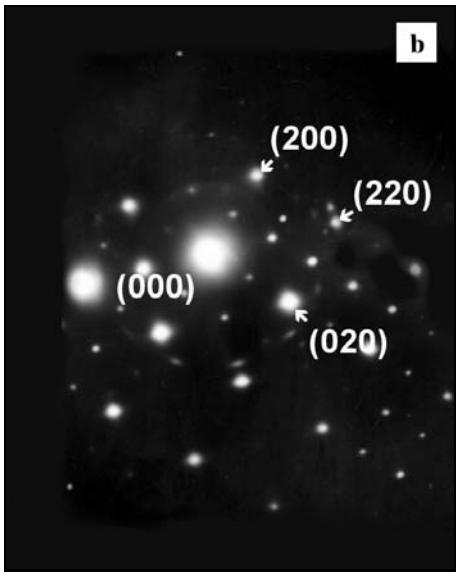

Fig. 9b. SAED pattern corresponding to $[0\,0\,\bar{1}]$ zone of γ-Ni/γ'-Ni_3Al.

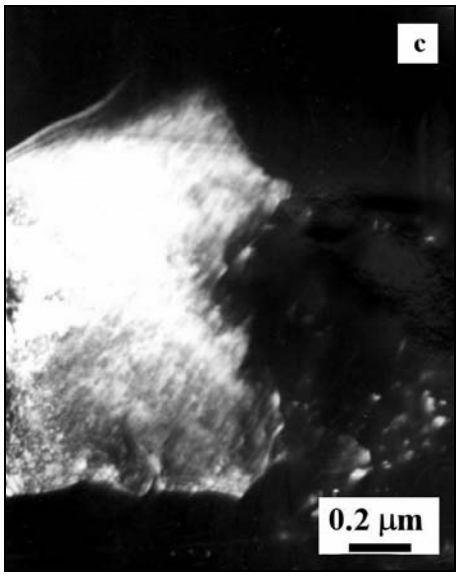

Fig. 9c. Dark field image formed using (1 1 0) reflection of γ'-Ni_3Al.

ations leading to the thermodynamic equilibrium in the coating are to be expected under exposure to elevated temperatures. These transformations are responsible

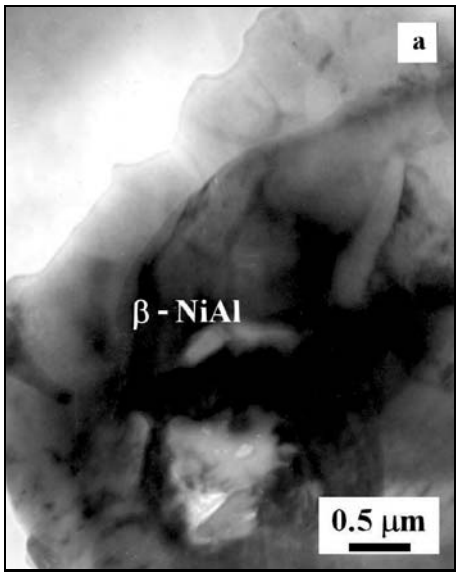

Fig. 10a. γ-Al_2O_3 oxide neighbouring the β-NiAl grain (TEM, BF image).

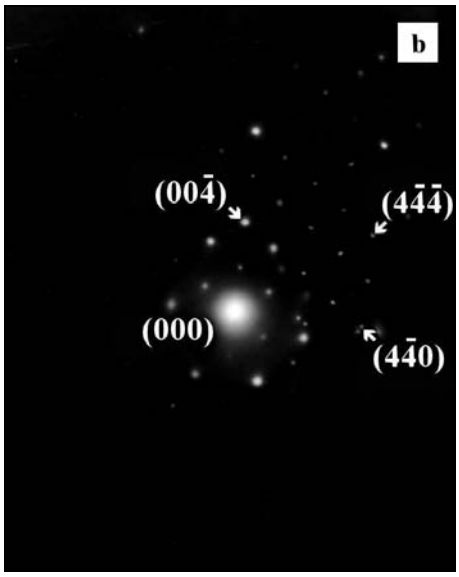

Fig. 10b. SAED pattern corresponding to [110] zone of γ-Al_2O_3.

Fig. 10c. Dark field image formed using $(1\,\bar{1}\,\bar{1})$ reflection of γ-Al_2O_3.

also for the dramatic average hardness increase from 130 HV 0.01 [1] to current 450 HV 0.01.

SEM observations and corresponding EDX analysis further confirmed that the transformation had resulted in the consumption of all Al rich regions. They were no more observed in the microstructure. Also the chemical composition is more homogeneous in the thermally exposed coating. With the exception of some primary γ-Ni grains, Al, and Ni atomic contents lie close together in the substantial part of the microstructure.

This was definitely approved by TEM analysis recognizing the equiatomic β-NiAl and martensitic NiAl as prevailing phases in the microstructure. The appearance of minor Al_3Ni and γ-Ni/γ'-Ni_3Al intermetallics can be accepted as a result of phase development governed mostly by the local chemistry. However, with respect to their scarce occurrence, it cannot be concluded whether they had appeared already during the APS or lately due to the thermal treatment. Generally, nearly complete transformation of metallic constituents of as-sprayed structure into intermetallic phases was confirmed by TEM. The observed orientation relationship between Al_3Ni and β-NiAl is based on the close interplanar distances of $(1\,\overline{2}\,1)$ of Al_3Ni, where $d_{(1\overline{2}1)} = 0.2675$ nm, and $(0\,1\,0)$ of β-NiAl, where $d_{(010)} = 0.2870$ nm.

As the APS coating was recognized as a mixture of different phases including α-Al, γ-Ni, intermetallic phases, and oxides, processes running at heating stage might have some similarity with those observed by heating of ball-milled Al-Ni elemental powder blends. These were extensively studied in numerous papers. Most of these studies were attracted by the mutual reaction between Al and Ni, exothermic in nature, that under circumstances takes place, opening thus, principally, new ways for economic production of the whole family of nickel aluminides [3–8].

It was repeatedly shown that this reaction is strongly affected by external pressure, heating rate, heat loss from the sample to the environment [9], atmosphere [10], by the presence of interfacial diffusion barriers [11], etc. The kinetics of the reaction is not understood in detail yet, however it is generally accepted, that the reaction may run in two different modes depending on the actual heating rate.

As reported by Plazanet and Nardou [12], for low heating rates ($< 5\ \mathrm{K\cdot min^{-1}}$) two weak exothermic peaks appear in the DTA curve. First peak starts at 535 ℃ and corresponds to $NiAl_3$ and Ni_2Al_3 formation. The second peak appears close to 638 ℃ what is the Ni-Al eutectic temperature. The reaction of $NiAl_3$ and Ni_2Al_3 formation is a solid-solid reaction. Ni_2Al_3 is developing as a dense layer at the Ni and Al grain interfaces making the reaction of these two elements difficult because of the lack of contacts. The reaction proceeds faster only above the eutectic temperature when $NiAl_3$ and Ni_2Al_3 phases react with the remaining nickel and aluminium. This reaction induces the appearance of the desired NiAl phase. However, the Ni is totally consumed from 1100 ℃.

In the case of heating rate higher than $5\ \mathrm{K\cdot min^{-1}}$, the direct synthesis of NiAl takes place via the thermal explosion [12]. DTA shows only one peak in this case. When the initial powder is not precompacted, the ignition temperature is higher

than for compacted samples. This is due to the numerous contacts between Ni and Al making the earlier start of the reaction possible. The reaction can be further powered by energy released by aluminium oxide formation triggering thus the NiAl synthesis.

The reaction during the heating up of NiAl coating displays features that might be attributed to both reaction modes. As only one exothermic peak is observed in the DTA curve and in particular NiAl phases can be found in the thermally treated microstructure – the reaction is similar to thermal explosion. On the other hand, minor amounts of retained γ-Ni indicate that the reaction has still not been fully completed and this is typical for the low heating rate mode.

As revealed by DTA, the reaction starts at relatively low temperature 490 °C what can be related to excellent metallurgical reactant contacts in the coating. This might be acknowledged as the beginning of reaction synthesis of NiAl phase. Really, no significant amounts of Ni_2Al_3 or Al_3Ni phases confirming the solid-solid reaction were found in the treated microstructure. However, the synthesis is not very intensive as the amounts of elemental Ni and Al available for the reaction are limited. This is because they were partially consumed already by preliminary reactions that took place during the APS process. This is also the reason, why the expected increase in porosity due to 14 % density increase upon NiAl formation from the elemental constituents [13] did not occur, as well.

Therefore the current reaction is restricted to certain locations with appropriate chemical and phase composition. These reaction sites are ignited by the energy input from the furnace and local reactions running in the neighbourhood. This process proceeds in the temperature range up to 730 °C where the coating reaches its new equilibrium. However, as some unreacted γ-Ni still remains in the coating, further transformations cannot be excluded. Heating up the samples to more elevated temperatures or isothermal exposure for longer periods of time should show whether this retained γ-Ni will transform into NiAl or some other phase, e.g., γ'-Ni_3Al. This might be the case, if too much Al has been already consumed by oxidation. However, the potential for any further thermal explosion seems to be exhausted.

No in-situ temperature measurements were performed in this experiment. However, the fact that exclusively crystalline oxides were found in the thermally treated coating indicates that a significant temperature increase had taken place during the exothermic reaction. The amorphous-crystalline transition of all amorphous oxides is assumed to be the result of this additional energy input. This can be concluded from the fact that analogous isothermal exposure of NiCrAlY APS coating reported in paper [14] did not lead to any transformation of amorphous oxides into crystalline structures.

5. Conclusions

The microstructure of NiAl APS coating isothermally exposed at 850 ℃ for 6 minutes in air was studied in this paper.

An exothermic reaction starting at 490 ℃ was determined within the heating period performed with the rate of 10 $K \cdot min^{-1}$.

The reaction was recognized as a reaction synthesis restricted to local areas with appropriate chemical and phase composition.

Metallic phases with the exception of some retained γ-Ni reacted to form NiAl phase.

Average microhardness of the coating increased from 130 to 450 HV 0.01.

The local temperature increase induced by the exothermic reaction is responsible for the amorphous-crystalline transition of all amorphous oxides.

Acknowledgements

The authors gratefully acknowledge the Scientific Grant Agency of the Ministry of Education of the Slovak Republic and Slovak Academy of Sciences (Grant project No. 2/4165/04) for the financial support of this work.

REFERENCES

[1] IŽDINSKÝ, K.—DUFEK, J.—IVAN, J.—ZEMÁNKOVÁ, M.—MINÁR, P.—IŽDINSKÁ, Z. : Kovove Mater., *41*, 2003, p. 365.
[2] IŽDINSKÝ, K.—IŽDINSKÁ, Z.—DUFEK, J.—IVAN, J.—ZEMÁNKOVÁ, M.: Kovove Mater., *41*, 2003, p. 106.
[3] MOORE, J. J.—FENG, J.: Progress in Mater. Sci., *39*, 1995, p. 243.
[4] MORSI, K.: Mater. Sci. Eng. A, *299*, 2001, p. 1.
[5] MIRACLE, D. B.: Acta Metall. Mater., *41*, 1993, p. 649.
[6] ATZMON, M.: Phys. Rev. Lett., *64*, 1990, p. 487.
[7] LAPIN, J.—WIERZBINSKI, S.—PELACHOVÁ, T.: Intermetallics, *7*, 1999, p. 705.
[8] LAPIN, J.: Kovove Mater., *40*, 2002, p. 209.
[9] ZHU, H. X.—ABBASCHIAN, R.: J. Mater. Sci., *38*, 2003, p. 3861.
[10] RABIN, B. H.—BOSE, A.—GERMAN, R. M.: Mod. Dev. Powd. Met., *20*, 1988, p. 511.
[11] ATZMON, M.: Metal. Trans., *23A*, 1992, p. 49.
[12] PLAZANET, L.—NARDOU, F.: J. Mater. Sci., *33*, 1998, p. 2129.
[13] VILLARS, P.—CALVERT, D.: Pearson's Handbook of Crystallographic Data for Intermetallic Phases. Metals Park, OH, ASM 1985.
[14] IŽDINSKÝ, K.—IVAN, J.—ZEMÁNKOVÁ, M.: Kovove Mater., *38*, 2000, p. 329.

Received: 1.4.2004